Biochemical and Biophysical Research Communications 456 (2015) 282–287

Contents lists available at ScienceDirect

Biochemical and Biophysical Research Communications

journal homepage: www.elsevier.com/locate/ybbrc

Thermodynamic parameters for binding of some halogenated inhibitors of human protein kinase CK2

Maria Winiewska [a], Małgorzata Makowska [a], Piotr Maj [a,b], Monika Wielechowska [c], Maria Bretner [c], Jarosław Poznański [a,*], David Shugar [a]

[a] Institute of Biochemistry and Biophysics PAS, Warszawa, Poland
[b] Nencki Institute of Experimental Biology PAS, Warszawa, Poland
[c] Warsaw University of Technology, Faculty of Chemistry, Warszawa, Poland

ARTICLE INFO

Article history:
Received 8 November 2014
Available online 25 November 2014

Keywords:
Protein kinase CK2
Bromobenzotriazoles
Bromobenzimidazoles
Halogenated protein ligands
DSC
Fluorescence

ABSTRACT

The interaction of human CK2α with a series of tetrabromobenzotriazole (**TBBt**) and tetrabromobenzimidazole (**TBBz**) analogs, in which one of the bromine atoms proximal to the triazole/imidazole ring is replaced by a methyl group, was studied by biochemical (IC_{50}) and biophysical methods (thermal stability of protein–ligand complex monitored by DSC and fluorescence). Two newly synthesized tri-bromo derivatives display inhibitory activity comparable to that of the reference compounds, **TBBt** and **TBBz**, respectively. DSC analysis of the stability of protein–ligand complexes shows that the heat of ligand binding (H_{bind}) is driven by intermolecular electrostatic interactions involving the triazole/imidazole ring, as indicated by a strong correlation between H_{bind} and ligand pK_a. Screening, based on fluorescence-monitored thermal unfolding of protein–ligand complexes, gave comparable results, clearly identifying ligands that most strongly bind to the protein. Overall results, additionally supported by molecular modeling, confirm that a balance of hydrophobic and electrostatic interactions contribute predominantly, relative to possible intermolecular halogen bonding, in binding of the ligands to the CK2α ATP-binding site.

1. Introduction

Protein kinase CK2 (casein kinase 2) is a kinase of widespread interest because of its role in control of numerous cellular functions. It is a constitutively active Ser/Thr protein kinase, also known to phosphorylate some Tyr residues. It is distributed ubiquitously in eukaryotic organisms, regulating hundreds of independent cellular processes – more than 300 protein substrates have been identified [1]. CK2 is involved, among others, in various signaling pathways, e.g. homeostasis maintenance and apoptosis [2], and there is a strong correlation between malignancy and an abnormally high activity of CK2 in cancer cells [3]. Hence, CK2 has become a therapeutic target for inhibitors directed to cancer treatment [4,5]. An increasing number of high-resolution structures of CK2-ligand complexes helps in *in silico* development of new CK2 inhibitors [6]. Many of them are halogenated, and recent studies demonstrate that halogen bonding, i.e. intermolecular interaction between ligand halogen atom(s) and protein electron-donating groups (e.g. carbonyl oxygens) may drive protein–ligand interactions [7–14]. The role of halogenated ligands in biological systems, has been extensively reviewed, among others, by Auffinger et al. [15], Voth & Ho [12], Parisini et al. [11], Grant & Lunney [16], Lu et al. [10], Rendine et al. [17] and Poznanski & Shugar [7,18]. However the free energy contribution of halogen bonding to protein–ligand interactions is debatable [18–20].

One of the first reported low-mass ATP-competitive inhibitors is 4,5,6,7-tetrabromo-1*H*-benzotriazole (**TBBt**, Scheme 1), which, when tested against a panel of more than 80 other kinases, displayed reasonably good selectivity for CK2 and its catalytic domain CK2α [4,5]. Subsequently, the closely related 4,5,6,7-tetrabromo-1*H*-benzimidazole (**TBBz**, Scheme 1) was also found to be a CK2α inhibitor. Both target the ATP-binding site [21,22], albeit their orientation within the pocket are visibly different (see Supplementary Fig. S1). More potent inhibitors have since been reported, many of them designed as **TBBt** and **TBBz** analogs [23,24]. Rational drug design is aided by a knowledge of the thermodynamics parameters that characterize interaction of ligands with a target protein. We have found that a balance of hydrophobic and electrostatic interactions, with eventual possible contribution of halogen bonding,

* Corresponding author at: Department of Biophysics, Institute of Biochemistry and Biophysics Polish Academy of Sciences, Pawińskiego 5a, 02-106 Warszawa, Poland.
E-mail address: jarek@ibb.waw.pl (J. Poznański).

http://dx.doi.org/10.1016/j.bbrc.2014.11.072
0006-291X/

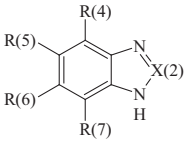

TBBt	R(4), R(5), R(6), R(7) = Br; X(2) = N
TBBz	R(4), R(5), R(6), R(7) = Br; X(2) = C
Br_3MeBt	R(4) = CH_3; R(5), R(6), R(7) = Br; X(2) = N
Br_3MeBz	R(4) = CH_3; R(5), R(6), R(7) = Br; X(2) = C
BrMeBt	R(4) = CH_3; R(5) = Br; R(6), R(7) = H; X(2) = N
BrMeBz	R(4) = CH_3; R(5) = Br; R(6), R(7) = H; X(2) = C

Scheme 1. Structures of tested inhibitors.

drive inhibitory activity of benzotriazoles halogenated on the benzene ring [25,26].

Herein, we analyze the activity and affinity of **TBBt**, **TBBz**, and two rationally selected methyl derivatives of each, in which the bromine atom at C(4) is replaced by a methyl group (Scheme 1). The inhibitory activities are compared with the thermodynamic parameters describing protein–ligand interactions, obtained by a DSC and fluorescence-monitored thermal unfolding. Two other derivatives, 5-bromo-4-methyl-Bt and 5-bromo-4-methyl-Bz, were studied as reference compounds that are structurally closely related, but differ substantially in their physico-chemical properties (size, hydrophobicity, pK_a).

2. Materials and methods

2.1. Chemistry

All reagents and solvents were commercially available (Aldrich, Avantor, Chempur, Merck). Melting points (uncorrected) were determined in open capillary tubes, using a Büchi apparatus B504. UV absorption spectra were recorded on a Specord 200 (AnalitykJena) or Cary 50 Bio instruments. Purity of all compounds was checked by thin-layer chromatography (TLC) on 0.2 mm Merck silica gel 60 F254 plates. Mass spectrometry was performed with a Micromass ESI Q-TOF spectrometer. ^{1}H and ^{13}C NMR spectra were recorded in DMSO-d_6 on Varian 500 or Bruker 300 instruments. Spectra were analyzed with the aid of the MestRe-C program [27]. Chemical shifts are relative to tetramethylsilane (Me_4Si, $\delta = 0$). The values of pK_a for dissociation of the triazole or imidazole proton were determined spectroscopically by analysis of pH-dependence of UV spectra in the range of 230–350 nm, assuming a two-state equilibrium between neutral and anionic forms (see [28] for details).

4,5,6,7-Tetrabromo-1*H*-benzotriazole (**TBBt**) and 4,5,6,7-tetrabromo-1*H*-benzimidazole (**TBBz**) were synthesized according to previously described procedures [29,30]. Compounds with methyl group in C(4) position and bromine atom in C(5) position or bromine atoms in positions C(5), C(6) and C(7) were synthesized from commercially available 2-bromo-6-nitrotoluene, which was, in the first step, selectively nitrated with urea nitrate [31] in sulfuric acid at 2 °C [32]. Reduction of the dinitro compound with tin (II) chloride in HCl [33] gave 2-bromo-5,6-diaminotoluene dihydrochloride, which reacted with sodium nitrite to yield 5-bromo-4-methyl-1*H*-benzotriazole (**BrMeBt**). The reaction of 2-bromo-5,6-diaminotoluene dihydrochloride with formic acid in 4 M HCl, under reflux, led to 5-bromo-4-methyl-1*H*-benzimidazole (**BrMeBz**). Bromination [29,30] of BrMeBt and BrMeBz gave, respectively, 4,5,6-tribromo-7-methyl-1*H*-benzotriazole (**Br_3MeBt**) and 4,5,6-tribromo-7-methyl-1*H*-benzimidazole (**Br_3MeBz**). Synthetic procedures are described in Supplementary materials.

2.2. CK2α phosphorylation assay – IC_{50} determination

CK2α was expressed and purified according to our published procedure [34]. An isotopic assay was used to determine CK2α activity using a synthetic peptide substrate (RRRDDDSDDD) from Biaffin GmbH & Co KG, Germany (see Supplementary for details). Experiments were carried out at 30 °C for 20 min in the presence of the increasing concentrations of inhibitors.

2.3. Differential scanning calorimetry (DSC)

Measurements were carried on a Nano DSC differential scanning calorimeter (TA Instruments) equipped with a cell of 300 μL volume. A pressure of 3 atm was applied to prevent vaporization upon heating. Protein thermal denaturation was monitored by the heat effect accompanying changes in heat capacity. The temperature was varied in the range 20–80 °C (1 °C/min). Protein concentrations were 0.4–0.6 mg/mL. Appropriate ligand solutions were used to obtain 1:1 ligand to protein ratios.

At midpoint temperature (T_m), $\Delta G_{unf}(T_m) = 0$, so $\Delta S_{unf}(T_m) = \Delta H_{unf}(T_m)/T_m$, where $\Delta H_{unf}(T_m)$ is the apparent heat of transition at T_m, deduced directly from a DSC thermogram (ΔH_{cal}). All these thermodynamic parameters were further extrapolated to 25 °C as follows:

$$\begin{aligned} \Delta H(T) &= \Delta H(T_m) + \Delta C_p \cdot (T - T_m) \\ \Delta S(T) &= \Delta S(T_m) + \Delta C_p \cdot \ln(T/T_m) \\ \Delta G(T) &= \Delta H(T) - T \cdot \Delta S(T) \end{aligned} \quad (1)$$

where change in heat capacity upon unfolding (ΔC_p) was assumed temperature-independent, the value of which at T_m was estimated directly from heat flow thermograms as the difference between high- and low-temperature asymptotes at T_m. Finally, entropy, enthalpy and free energy for ligand binding were calculated as the difference between appropriate thermodynamic parameters estimated separately for free and ligand-bound protein.

2.4. Temperature-dependent fluorescence

Fluorescence data were collected on a Varian Cary Eclipse spectrofluorometer equipped with a constant-temperature cell holder, using 10-mm path-length cuvettes. Protein emission was monitored at 335 nm (excitation at 280 nm) at temperatures of 20–80 °C, with 1 °C/min heating rate. The protein was diluted to a final concentration of 0.3 μM with 25 mM Tris–HCl (pH 7.9), 0.6 M NaCl, 1 mM DTT and 20% glycerol. All ligand solutions were initially prepared in dimethyl sulfoxide (DMSO). Appropriate amounts of ligand stock solutions were diluted with DMSO and added to the protein sample to obtain the required ligand concentration, with a final DMSO concentration of 2%.

The simplest model for thermal unfolding of a protein assumes a two-state process driven by the equilibrium of the folded, F, and unfolded, U, protein forms. Thermodynamic parameters may be determined by fitting the appropriate model to the experimentally observed temperature-dependent intensity of protein fluorescence, $I_F(T)$. However, hCK2α unfolds irreversibly at elevated temperature, hence derived parameters may be highly biased. Consequently, the midpoint of thermal denaturation, T_m, is the only thermodynamic parameter that can be accurately determined according to the simplified Eq. (2):

$$I(T) = \frac{I_U(T) + I_F(T) \cdot e^{(T_m - T)\cdot p}}{1 + e^{(T_m - T)\cdot p}} \quad (2)$$

where p mimics the slope of $I(T)$ at T_m, and $I_F(T)$ and $I_U(T)$ are quadratic approximates of the temperature-dependence of fluorescence intensities of the folded (F) and unfolded (U) states, respectively. Parameter p roughly estimates heat of unfolding, (ΔH_{unf}).

2.5. Data analysis

Numerical models were fitted to experimental data, using the Marquardt algorithm [35] implemented in the GnuPlot program [36].

3. Results

3.1. Phosphorylation assay – in vitro determination of inhibitory activity against hCK2α

IC_{50} values for inhibition of hCK2α by **TBBt**, the two methylbromobenzotriazoles, and their benzimidazole analogs, are presented in Table 1. The representative dose–response curves are presented in Supplementary Fig. S2. In agreement with literature data, **TBBt** was found a visibly better inhibitor than **TBBz** [30]. Replacement of the bromine proximal to the triazole/imidazole ring by a methyl group results in a moderate decrease of inhibitory activity. However, this effect is stronger for **Br_3MeBz** (IC_{50} 3-fold higher than that of **TBBz**) than for **Br_3MeBt** (10% increase in IC_{50} relative to **TBBt**).

3.2. Differential scanning calorimetry (DSC)

Thermal denaturation of hCK2α and six 1:1 ligand–protein complexes was monitored with the aid of differential scanning calorimetry (DSC). This technique enables direct measurement of heat capacity (C_p), and simultaneous detection of transition temperature(s) (T_m) and associated heat(s) of unfolding (ΔH_{cal}). Both T_m and ΔH_{cal} can be obtained directly from the corrected thermogram as the location of the maximum, and area under the heat-flow curve (see Fig. 1A and B), after correction for low- and high-temperature C_p asymptotes. The resulting thermodynamic parameters are collected in Table 2.

All complexes are much more stable (i.e. display higher T_m values) than free hCK2α, clearly indicating that all ligands preferably bind to the folded protein. And generally, the higher the T_m with a given ligand, the more efficient it is as an inhibitor. Albeit, small differences in the individual $\Delta C_p(T)$, characterizing the balance of protein–ligand and solvent-ligand interactions, make the latter rule rather semiquantitative, as observed for **BrMeBt** and **Br_3MeBt**, which display almost identical T_m, but visibly different IC_{50} values.

Interestingly, heats of unfolding at T_m, as well as free energy of ligand binding extrapolated to 25 °C, are strictly related to the number of halogen atoms attached to the benzene ring of the benzotriazole/benzimidazole derivatives. This effect should be assigned to modulation of electrostatic interactions, rather than to an eventual contribution of halogen bonds, as clearly shown by the strong correlation between H_{cal} with pK_a values for dissociation of the ligand imidazole/triazole proton (Fig. 1C, see Scheme 1 for structures). It is worth noting that all benzotriazoles ionized at neutral pH display at ~50 °C a higher heat of dissociation than their benzimidazole analogs. This points directly to the effect of electrostatic interactions: all brominated benzotriazoles are much more polar than the corresponding benzimidazoles.

Table 1
In vitro CK2a inhibition by halogenated benzotriazole and benzimidazole derivatives. hCK2α activity expressed as percentage of the control activity in the presence of 5 μM inhibitor.

Compound	pK_a	IC_{50} (μM)	hCK2α activity (%)
BrMeBt	7.72	17.1 ± 1.3	73.5
Br_3Me-Bt	6.28	0.60 ± 0.13	8.9
TBBt	4.78 [26]	0.52 ± 0.06; 0.61 ± 0.09 [25]; 0.27 ± 0.07 [38]; 0.50 ± 0.07 [39]	5.1
BrMeBz	6.35; 11.77	Inactive	~100
Br_3MeBz	10.33	5.6 ± 1.2	50.3
TBBz	8.9 [40]	1.6 ± 0.4; 1.50 ± 0.14 [39]; 1.30 ± 0.23 [41]	20.9

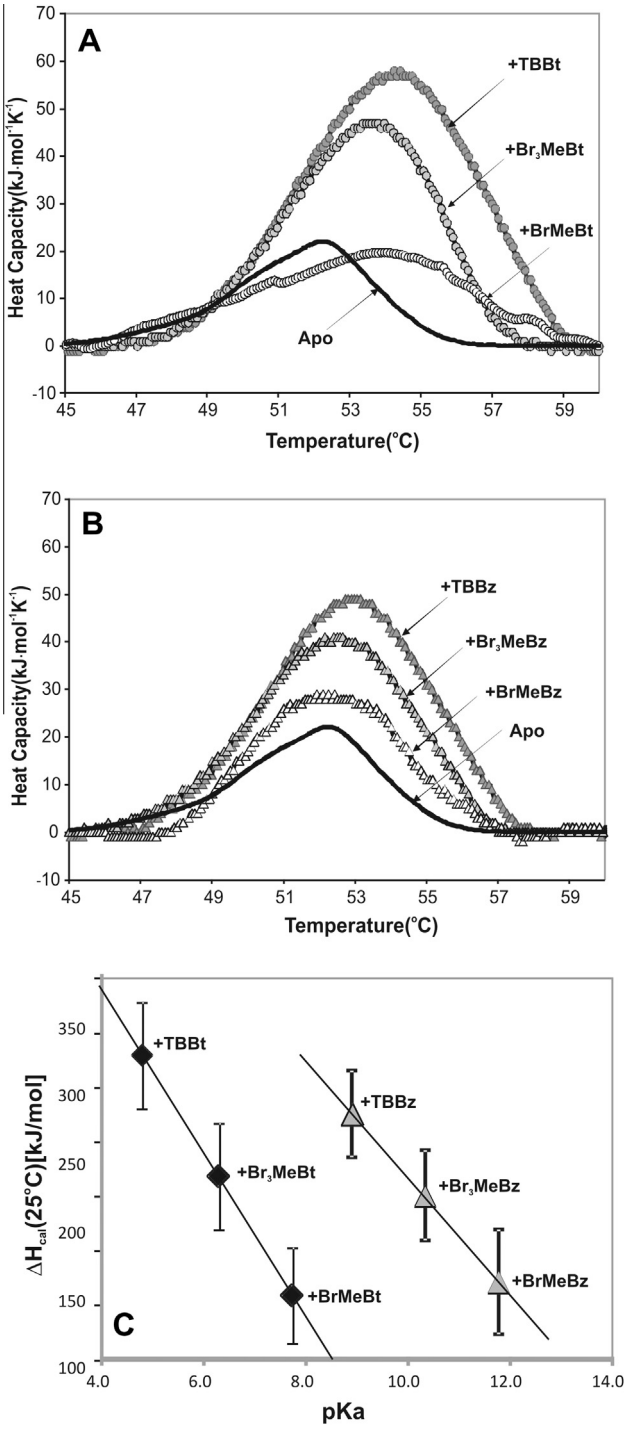

Fig. 1. DSC thermograms of hCK2α (solid line) and its 1:1 complexes with halogenated benzotriazoles (A) and benzimidazoles (B). Additionally, correlation between DSC-derived heats of unfolding and pK_a for dissociation of the ligand triazole/imidazole proton are presented (C).

3.3. Fluorescence-monitored melting of 1:1 ligand:protein complexes

The models fitted to the data for thermal unfolding of hCK2α and its 1:1 complexes with the six ligands are presented in

Table 2
Thermodynamic parameters obtained from DSC measurements for thermal unfolding of hCK2α and its 1:1 complexes.

Ligand	T_m (°C)	$\Delta H_{unf}(T_m)$ (kJ/mol)	ΔH_{unf}(25 °C) (kJ/mol)	ΔG_{unf}(25 °C) (kJ/mol)	ΔG_{diss}(25 °C) (kJ/mol)	K_{diss}(25 °C) (nM)
–	51.80 ± 0.03	121 ± 7	83 ± 13	8.4 ± 0.8	–	–
BrMeBt	53.41 ± 0.06	169 ± 16	129 ± 22	12.8 ± 1.7	33.9 ± 2.5	1220 ± 430
Br$_3$MeBt	53.26 ± 0.05	257 ± 20	217 ± 26	20.3 ± 2.0	41.4 ± 2.8	58 ± 28
TBBt	54.08 ± 0.03	346 ± 20	305 ± 26	28.7 ± 2.1	49.8 ± 2.9	2.1 ± 1.0
BrMeBz	52.37 ± 0.02	178 ± 19	139 ± 25	13.2 ± 1.5	34.3 ± 2.7	1010 ± 420
Br$_3$MeBz	52.44 ± 0.04	241 ± 14	202 ± 20	18.5 ± 1.5	39.6 ± 2.3	118 ± 30
TBBz	52.71 ± 0.04	301 ± 13	262 ± 19	23.8 ± 1.4	44.8 ± 2.2	14.5 ± 3.3

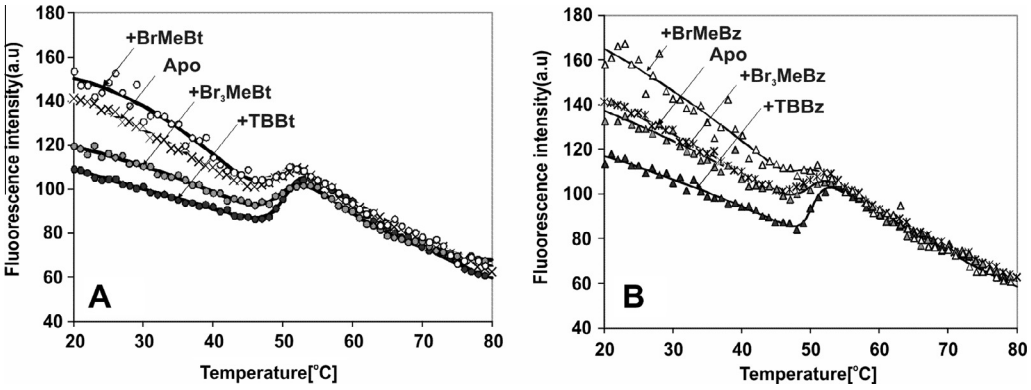

Fig. 2. Temperature-dependence of fluorescence intensity. Data recorded for CK2α (white squares) and its complexes with three halogenated benzotriazoles (A) and their bezimidazole analogs (B). Solid lines represent models fitted according to Eq. (2).

Table 3
Parameters for thermal unfolding of CK2α and its complexes with three halogenated benzotriazoles and their benzimidazole analogs. I_0 is the estimated fluorescence of the protein at 20 °C, and T_m, $\Delta I(T_m)$ and p represent the melting temperature, change in fluorescence upon thermal denaturation, and a rough estimate of the heat of unfolding, respectively (see Eq. (2)).

Ligand	T_m (°C)	I_0 (20 °C)	$\Delta I(T_m)$	p (K^{-1})
–	48.73 ± 0.25	142.42 ± 1.58	14.72 ± 0.80	4.45 ± 0.84
BrMeBt	48.94 ± 0.51	150.40 ± 10.76	4.46 ± 1.36	4.08 ± 1.30
Br$_3$MeBt	50.38 ± 0.34	121.50 ± 0.03	11.54 + 0.77	5.24 ± 0.70
TBBt	50.70 ± 0.14	108.79 ± 0.06	27.07 ± 0.36	6.99 ± 1.10
BrMeBz	48.89 ± 1.05	164.76 ± 48.27	2.38 ± 2.80	5.38 ± 4.39
Br$_3$MeBz	49.96 ± 0.61	136.96 ± 18.94	9.72 ± 1.75	4.63 ± 2.02
TBBz	50.40 ± 0.19	116.98 ± 12.95	23.65 ± 0.52	5.83 ± 0.96

Fig. 2A and B for benzotriazoles and benzimidazoles, respectively. A common trend of $I_F(T)$, observed for all six complexes at the high-temperature region ($T > 55$ °C), which is close to that observed for the free protein, clearly indicates that none of the ligands binds effectively to an unfolded form of hCK2α. Inspection of the values of the fitted parameters presented in Table 3 confirms that binding of four ligands (**TBBt**, **TBBz**, **Br$_3$MeBt** and **Br$_3$MeBz**) results in a significant increase of T_m, relative to the *apo* protein (see also Fig. 2), so that the structure of hCK2α is stabilized when each of these ligands is bound. Binding of these ligands also results in significant quenching of tyrosine fluorescence, most putatively Tyr50 of hCK2α, corresponding to the Tyr50 of maize CK2α, which is located within 10 Å of a ligand in the crystal structures of maize CK2α with **TBBt** and **TBBz** (PDB entries 1j91 [22] and 2oxy [37], respectively (see Supplementary Fig. S1). Binding of **Br$_3$MeBz** results in a smaller shift of T_m, but, in contrast to **TBBt**, **TBBz** and **Br$_3$MeBt**, its binding only slightly decreases tyrosine fluorescence of the protein folded state. This indicates that **Br$_3$MeBz** may bind in a different orientation than **TBBt** and **TBBz**. Finally, virtually no stabilization is observed with **BrMeBt** and **BrMeBz**, confirming again that these two compounds are very weak CK2α inhibitors that do not efficiently bind at the 200 pM concentration used in the fluorescence assay.

4. Discussion

Both calorimetry and fluorescence techniques identified the most active inhibitors, and properly order their activity within the series of either triazoles or imidazoles. It should be stressed that the binding of brominated benzotriazole/benzimidazole to hCK2α is driven by a balance of electrostatic and hydrophobic interactions. We have recently shown that, among ligands displaying similar electronic properties (i.e. close pK_a for dissociation of the triazole/imidazole proton), those carrying the larger number of halogens are the most active. And for **TBBt**-derived ligands with the same number of bromines, that with the highest pK_a is the strongest hCK2α inhibitor [38]. Indeed, a general correlation presented in Fig. 3 validates the relation between pK_a for dissociation of the triazole proton and inhibitory activity. The almost horizontal line follows the trend observed for compounds that carry the same number of Br atoms attached to C(5)/C(6), but differ by the number of Br atoms attached to C(4)/C(7). Bromination of both C(5) and C(6) carbons appears to be crucial for efficient interaction of halogenated benzotriazole derivatives with CK2α. In agreement with the foregoing, the inhibitory activity of **Br$_3$MeBt** (IC_{50} = 0.60 ± 0.13 μM, gray circle in Fig. 3) is close to that of 4,5,6-Br$_3$Bt (0.38 ± 0.02 μM), since both compounds are of comparable hydrophobicity and with almost identical pK_a. With the benzimidazole derivatives, replacement of a single bromine atom of **TBBz** by a methyl group also results in a decrease of hydrophobicity. However, contrary to halogenated benzotriazoles, an increase in pK_a for halogenated benzimidazoles (10.3 vs 8.9) does not significantly change the protonation equilibrium at the physiological pH of 7.5 used in the enzymatic assay. Consequently, the loss in hydrophobicity cannot be compensated for by an increase of electrostatic interactions, and **Br$_3$MeBz** is visibly less active than **TBBz**. The foregoing is also valid for methylated derivatives of monobrominated Bt and Bz. Thus, **BrMeBt** (IC_{50} = 17.1 ± 1.3 μM) is even more active than its non-methylated analog, 5-BrBt (IC_{50} = 26 ± 3 μM), the pK_a of which is visibly lower (7.55 vs 7.72 for **BrMeBt**). And, finally, **BrMeBz** is virtually inactive.

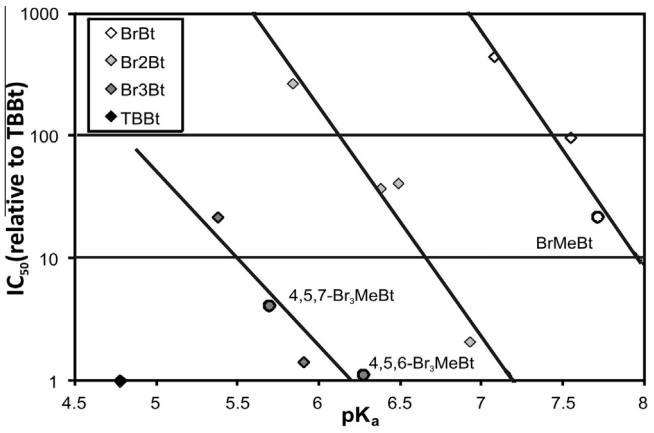

Fig. 3. Schematic representation of the effects of bromination of the benzene ring of benzotriazole (**Bt**), including interdependence of the pK_a of the products with their IC_{50} for inhibition of protein kinase hCK2α. Black lines link products with the same number of bromine atoms, but substantially differing in pK_a and IC_{50}. Horizontal line marks the di- and tri-brominated derivatives with inhibitory activities comparable to that of **TBBt**. The IC_{50} scale is relative to **TBBt** activity measured as the reference.

Overall, this confirms our finding that bromination at C(5) and C(6) of the benzene ring of benzotriazole is crucial for inhibitory activity, while substituents at C(4) and C(7) can be further modified. Herein, we show that replacement of one "unfavorable" bromine atom, that at C(4), by a methyl group clearly enhances inhibitory activity (see circles in Fig. 3).

The eventual role of putative halogen bonding remains unanswered. Based on X-ray structures of **TBBz** and **TBBt** with maize CK2α (see Supplementary Fig. 1), one may expect that replacement of one bromine atom by a methyl group should not interfere with halogen-bonding interactions of **Br_3MeBz** with the protein via Br(5) and Br(6), contrary to **Br_3MeBt** complex in which a halogen bond between C(4)/C(7) of **TBBt** and either carbonyl oxygen or sidechain Nε of Arg47 might be disrupted. However, experimental data show the opposite effect: binding, and activity, are much more decreased with **Br_3MeBz** than with **Br_3MeBt**. Moreover, the observed correlation between the DSC-derived enthalpies and ligand pK_a strongly supports a predominance of direct hydrogen bonding/electrostatic interactions involving the triazole ring.

Finally, it should be noted that in physiological conditions **Br_3MeBt** is visibly less dissociated than **TBBt**, what may decrease the undesired side-effect of mitochondrial membrane depolarization observed for **TBBt** [24], which is anionic in physiological conditions.

Acknowledgments

This work was supported by the Polish National Centre for Science grants 2011/01/B/ST5/ 00849 (to M.B.) and 2012/07/B/ST4/ 01334 (to J.P.) and Warsaw University of Technology. The equipment used was sponsored in part by the Centre for Preclinical Research and Technology (CePT), a project co-sponsored by European Regional Development Fund and Innovative Economy, The National Cohesion Strategy of Poland.

Appendix A. Supplementary data

Supplementary data associated with this article can be found, in the online version, at http://dx.doi.org/10.1016/j.bbrc.2014.11.072.

References

[1] F. Meggio, L.A. Pinna, One-thousand-and-one substrates of protein kinase CK2?, FASEB J 17 (2003) 349–368.
[2] D.W. Litchfield, Protein kinase CK2: structure, regulation and role in cellular decisions of life and death, Biochem. J. 369 (2003) 1–15.
[3] S. Tawfic, S. Yu, H. Wang, R. Faust, A. Davis, K. Ahmed, Protein kinase CK2 signal in neoplasia, Histol. Histopathol. 16 (2001) 573–582.
[4] M.A. Pagano, J. Bain, Z. Kazimierczuk, S. Sarno, M. Ruzzene, G. Di Maira, M. Elliott, A. Orzeszko, G. Cozza, F. Meggio, L.A. Pinna, The selectivity of inhibitors of protein kinase CK2: an update, Biochem. J. 415 (2008) 353–365.
[5] S. Sarno, E. Papinutto, C. Franchin, J. Bain, M. Elliott, F. Meggio, Z. Kazimierczuk, A. Orzeszko, G. Zanotti, R. Battistutta, L.A. Pinna, ATP site-directed inhibitors of protein kinase CK2: an update, Curr. Top. Med. Chem. 11 (2011) 1340–1351.
[6] K. Niefind, J. Raaf, O.G. Issinger, Protein kinase CK2: from structures to insights, Cell. Mol. Life Sci. 66 (2009) 1800–1816.
[7] J. Poznanski, D. Shugar, Halogen bonding at the ATP binding site of protein kinases: preferred geometry and topology of ligand binding, Biochim. Biophys. Acta Proteins Proteomics 2013 (1834) 1381–1386.
[8] M.O. Zimmermann, A. Lange, R. Wilcken, M.B. Cieslik, T.E. Exner, A.C. Joerger, P. Koch, F.M. Boeckler, Halogen-enriched fragment libraries as chemical probes for harnessing halogen bonding in fragment-based lead discovery, Future Med. Chem. 6 (2014) 617–639.
[9] Z. Xu, Z. Yang, Y. Liu, Y. Lu, K. Chen, W. Zhu, Halogen bond: its role beyond drug-target binding affinity for drug discovery and development, J. Chem. Inf. Model. 54 (2014) 69–78.
[10] Y. Lu, Y. Liu, Z. Xu, H. Li, H. Liu, W. Zhu, Halogen bonding for rational drug design and new drug discovery, Expert Opin. Drug Discov. 7 (2012) 375–383.
[11] E. Parisini, P. Metrangolo, T. Pilati, G. Resnati, G. Terraneo, Halogen bonding in halocarbon–protein complexes: a structural survey, Chem. Soc. Rev. 40 (2011) 2267–2278.
[12] A.R. Voth, P.S. Ho, The role of halogen bonding in inhibitor recognition and binding by protein kinases, Curr. Top. Med. Chem. 7 (2007) 1336–1348.
[13] R. Wilcken, M.O. Zimmermann, A. Lange, A.C. Joerger, F.M. Boeckler, Principles and applications of halogen bonding in medicinal chemistry and chemical biology, J. Med. Chem. 56 (2013) 1363–1388.
[14] L.A. Hardegger, B. Kuhn, B. Spinnler, L. Anselm, R. Ecabert, M. Stihle, B. Gsell, R. Thoma, J. Diez, J. Benz, J.-M. Plancher, G. Hartmann, D.W. Banner, W. Haap, F. Diederich, Systematic investigation of halogen bonding in protein–ligand interactions, Angew. Chem. Int. Ed. 50 (2011) 314–318.
[15] P. Auffinger, F.A. Hays, E. Westhof, P.S. Ho, Halogen bonds in biological molecules, Proc. Natl. Acad. Sci. U.S.A. 101 (2004) 16789–16794.
[16] S.K. Grant, E.A. Lunney, Kinase inhibition that hinges on halogen bonds, Chem. Biol. 18 (2011) 3–4.
[17] S. Rendine, S. Pieraccini, A. Forni, M. Sironi, Halogen bonding in ligand–receptor systems in the framework of classical force fields, Phys. Chem. Chem. Phys. 13 (2011) 19508–19516.
[18] J. Poznanski, A. Poznanska, D. Shugar, A protein data bank survey reveals shortening of intermolecular hydrogen bonds in ligand–protein complexes when a halogenated ligand is an H-bond donor, PLoS One 9 (2014) e99984.
[19] M. Carter, P.S. Ho, Assaying the energies of biological halogen bonds, Cryst. Growth Des. 11 (2011) 5087–5095.
[20] C.B. Aakeroey, S. Panikkattu, P.D. Chopade, J. Desper, Competing hydrogen-bond and halogen-bond donors in crystal engineering, CrystEngComm 15 (2013) 3125–3136.
[21] S. Sarno, H. Reddy, F. Meggio, M. Ruzzene, S.P. Davies, A. Donella-Deana, D. Shugar, L.A. Pinna, Selectivity of 4,5,6,7-tetrabromobenzotriazole, an ATP site-directed inhibitor of protein kinase CK2 ('casein kinase-2'), FEBS Lett. 496 (2001) 44–48.
[22] R. Battistutta, E. De Moliner, S. Sarno, G. Zanotti, L.A. Pinna, Structural features underlying selective inhibition of protein kinase CK2 by ATP site-directed tetrabromo-2-benzotriazole, Protein Sci. 10 (2001) 2200–2206.
[23] S. Sarno, M. Ruzzene, P. Frascella, M.A. Pagano, F. Meggio, A. Zambon, M. Mazzorana, G. Di Maira, V. Lucchini, L.A. Pinna, Development and exploitation of CK2 inhibitors, Mol. Cell. Biochem. 274 (2005) 69–76.
[24] M.A. Pagano, M. Andrzejewska, M. Ruzzene, S. Sarno, L. Cesaro, J. Bain, M. Elliott, F. Meggio, Z. Kazimierczuk, L.A. Pinna, Optimization of protein kinase CK2 inhibitors derived from 4,5,6,7-tetrabromobenzimidazole, J. Med. Chem. 47 (2004) 6239–6247.
[25] R. Wasik, M. Lebska, K. Felczak, J. Poznanski, D. Shugar, Relative role of halogen bonds and hydrophobic interactions in inhibition of human protein kinase CK2 alpha by tetrabromobenzotriazole and some C(5)-substituted analogues, J. Phys. Chem. B 114 (2010) 10601–10611.
[26] R. Wasik, P. Winska, J. Poznanski, D. Shugar, Synthesis and physico-chemical properties in aqueous medium of all possible isomeric bromo analogues of benzo-1H-triazole, potential inhibitors of protein kinases, J. Phys. Chem. B 116 (2012) 7259–7268.
[27] J.C. Cobas, F.J. Sardina, Nuclear magnetic resonance data processing. MestRe-C: a software package for desktop computers, Concepts Magn. Reson. Part A 19A (2003) 80–96.
[28] J. Poznanski, A. Najda, M. Bretner, D. Shugar, Experimental (C-13 NMR) and theoretical (ab initio molecular orbital calculations) studies on the prototropic tautomerism of benzotriazole and some derivatives symmetrically substituted on the benzene ring, J. Phys. Chem. A 111 (2007) 6501–6509.
[29] P. Borowski, J. Deinert, S. Schalinski, M. Bretner, K. Ginalski, T. Kulikowski, D. Shugar, Halogenated benzimidazoles and benzotriazoles as inhibitors of the NTPase/helicase activities of hepatitis C and related viruses, Eur. J. Biochem. 270 (2003) 1645–1653.
[30] P. Zien, M. Bretner, K. Zastapilo, R. Szyszka, D. Shugar, Selectivity of 4,5,6,7-tetrabromobenzimidazole as an ATP-competitive potent inhibitor of protein

kinase CK2 from various sources, Biochem. Biophys. Res. Commun. 306 (2003) 129–133.
[31] A.I. Vogel, A Textbook of Practical Organic Chemistry, third ed., Longman, London, 1971.
[32] S.R. Mundla, Regioselective synthesis of 4-halo ortho-dinitrobenzene derivatives, Tetrahedron Lett. 41 (2000) 4277–4279.
[33] A. Bettelheim, B.A. White, S.A. Raybuck, R.W. Murray, Electrochemical polymerization of amino-substituted, pyrrole-substituted, and hydroxyl substituted tetraphenylporphyrins, Inorg. Chem. 26 (1987) 1009–1017.
[34] P. Borowiecki, A.M. Wawro, P. Wińska, M. Wielechowska, M. Bretner, Synthesis of novel chiral TBBt derivatives with hydroxyl moiety. Studies on inhibition of human protein kinase CK2α and cytotoxicity properties, Eur. J. Med. Chem. 84 (2014) 364–374.
[35] D.W. Marquardt, An algorithm for least-squares estimation of nonlinear parameters, J. Soc. Ind. Appl. Math. 11 (1963) 431–441.
[36] T. Williams, C. Kelley, http://www.gnuplot.info, (2007).
[37] R. Battistutta, M. Mazzorana, L. Cendron, A. Bortolato, S. Sarno, Z. Kazimierczuk, G. Zanotti, S. Moro, L.A. Pinna, The ATP-binding site of protein kinase CK2 holds a positive electrostatic area and conserved water molecules, ChemBioChem 8 (2007) 1804–1809.
[38] R. Wasik, P. Winska, J. Poznanski, D. Shugar, Isomeric mono-, di-, and tri-bromobenzo-1H-triazoles as inhibitors of human protein kinase CK2 alpha, PLoS One 7 (2012) e48898.
[39] M. Bretner, A. Najda-Bernatowicz, M. Lebska, G. Muszynska, A. Kilanowicz, A. Sapota, New inhibitors of protein kinase CK2, analogues of benzimidazole and benzotriazole, Mol. Cell. Biochem. 316 (2008) 87–89.
[40] P. Zien, J.S. Duncan, J. Skierski, M. Bretner, D.W. Litchfield, D. Shugar, Tetrabromobenzotriazole (TBBt) and tetrabromobenzimidazole (TBBz) as selective inhibitors of protein kinase CK2: evaluation of their effects on cells and different molecular forms of human CK2, Biochim. Biophys. Acta Proteins Proteomics 1754 (2005) 271–280.
[41] A. Najda-Bernatowicz, M. Lebska, A. Orzeszko, K. Kopanska, E. Krzywinska, G. Muszynska, M. Bretner, Synthesis of new analogs of benzotriazole, benzimidazole and phthalimide-potential inhibitors of human protein kinase CK2, Bioorg. Med. Chem. 17 (2009) 1573–1578.